

General Disclaimer

One or more of the Following Statements may affect this Document

- This document has been reproduced from the best copy furnished by the organizational source. It is being released in the interest of making available as much information as possible.
- This document may contain data, which exceeds the sheet parameters. It was furnished in this condition by the organizational source and is the best copy available.
- This document may contain tone-on-tone or color graphs, charts and/or pictures, which have been reproduced in black and white.
- This document is paginated as submitted by the original source.
- Portions of this document are not fully legible due to the historical nature of some of the material. However, it is the best reproduction available from the original submission.

NASA CR-175150



(NASA-CR-175150) EARTH STRAIN MEASUREMENTS
WITH THE TRANSPORTABLE LASER RANGING SYSTEM:
FIELD TECHNIQUES AND PLANNING Final Report,
Dec. 1979 - Nov. 1982 (Texas Univ.) 42 p
HC A03/MF A01

N84-17725

Unclas

CSCL 08G G3/46 12212



THE UNIVERSITY OF TEXAS AT AUSTIN
Institute For Geophysics

EARTH STRAIN MEASUREMENTS
WITH THE TRANSPORTABLE LASER RANGING SYSTEM:
FIELD TECHNIQUES AND PLANNING

Yosio Nakamura
H. James Dorman
Thomas Cahill

The University of Texas at Austin
Institute for Geophysics
Galveston Marine Geophysics Laboratory
700 The Strand
Galveston, Texas 77550-2768

November 1982
Final Report for Period December 1979 - November 1982
NASA Contract NAS5-25897

Prepared for
GODDARD SPACE FLIGHT CENTER
Greenbelt, Maryland 20771
Technical Officer: Christopher C. Stephanides, Code 942

The University of Texas Institute for Geophysics
Contribution No. 532

ABSTRACT

We have conducted a feasibility study to examine the potential of the Transportable Laser Ranging System (TLRS) for monitoring the ground deformation around satellite ranging stations and other geodetic control points. Emphasis has been placed on testing the usefulness of the relative lateration technique. The temporal variation of the ratio of the length of each survey line to the mean length of all survey lines in a given area is directly related to the mean shear strain rate for the area. The data from a series of experimental measurements taken over the Los Angeles basin from a TLRS station at Mt. Wilson show that such ratios can be determined to an accuracy of one part in 10^7 with a measurement program lasting for three days and without using any corrections for variations in atmospheric conditions. A numerical experiment using a set of hypothetical data indicates that reasonable estimates of the present shear strain rate and the direction of the principal axes in southern California can be deduced from such measurements over an interval of one to two years. Thus, the relative lateration from the TLRS appears to be a very economical way to monitor ground deformations, although there has been no opportunity yet to measure the actual ground strain by reoccupying the Mt. Wilson site.

Table of Contents

I.	Introduction.....	1
II.	TLRS Ground-to-Ground Ranging.....	3
	Advantages and Problems.....	3
	Relative Lateration.....	4
	Relationship between Relative Lateration and Strain.....	4
III.	Mt. Wilson Experiment.....	9
	Field Experiment.....	9
	The Data.....	12
	Range Ratios to a Single Reference Line.....	12
	Time-of-Flight Ratios to the Mean.....	14
	An Alternative Atmospheric Correction.....	14
	A Test for Systematic Error Due to Atmospheric Conditions.....	17
	Results.....	19
IV.	Shear Strain Determination using Hypothetical Data.....	21
V.	Conclusions and Recommendations.....	22
	Conclusions.....	23
	Recommendations.....	23
	Acknowledgements.....	24
	References.....	25
	Appendix.....	26

I. INTRODUCTION

With the recent development in ground-to-satellite laser ranging and Very Long Baseline Interferometry (VLBI) techniques, it is now possible to measure precisely distances between locations separated by several hundreds to thousands of kilometers. This makes it possible to monitor relative movements of globally distributed points on the earth for geodynamic studies. However, one question that must be answered is how representative each of these positions thus occupied is for the region in which it is located. If some of these locations are experiencing localized movements which are not representative of the region, the global measurement would give erroneous results. An answer to this questions can be found by measuring regional deformations around each location.

A conventional method for determining regional deformations is to perform repeated survey using an electro-optical distance measuring (EDM) device (e.g. Savage et al. [1981]). However, such surveys are expensive, and are rather limited in range. We, therefore, have looked for a better alternative. The development of the Transportable Laser Ranging System (TLRS) for ground-to-LAGEOS (Laser Geodynamics Earth Orbiting Satellite) ranging [Silverberg and Byrd, 1981] has given us an opportunity to test such an alternative. Because of its high sensitivity, being capable of detecting single photon returns, the TLRS can measure distances to small targets (retro-reflectors) at any visible points much beyond the normal ranges of other EDM devices. Thus, this system may provide economical measurements of strain fields in areas more than 200 km in diameter. If successful, such measurements will be valuable not only in the immediate neighborhood of satellite ranging stations, but also in understanding the dynamic behavior of both plate boundaries and areas internal to plates.

We have conducted a limited feasibility study to examine this potential. Although the TLRS is a powerful system, it also has certain limitations when used for a ground-to-ground ranging. The most important is the uncertainty of measurement results due to variability in atmospheric conditions. To bypass this problem and avoid the expense of flying an aircraft to monitor the atmospheric conditions along the path of the laser beam, we have examined the use of the relative lateralization, or the ratio method, which was used earlier by Carter and Vincenty [1978] in an experimental survey around the McDonald Observatory.

We originally planned repeated field experiments at several sites in the western United States. However, because of many scheduling conflicts and delays associated with the overall TLRS-LAGEOS ranging experiments, the only field experiment we could perform during the current contract was a four-day measurement at Mt. Wilson over the Los Angeles basin in January, 1981. We have been unable to reoccupy this site for an actual strain measurement.

The present study, however, has given us some very encouraging results. Even with no atmospheric correction at all, the range ratios could be determined to an accuracy of one part in 10^7 . This is sufficient for an order-of-magnitude estimate of incremental shear strain in the southern California region if two measurements separated by one to two years are available. Higher accuracies would be attainable with repeated measurements.

In this report, we first describe the advantages and problems of ground-to-ground ranging by a TLRS, leading to the use of relative lateration, or range-ratio method, and its relationship to the regional strain (Section II). Then, we present the data and analysis of the Mt. Wilson experiment (Section III). This is followed by a short treatment of regional strain determination using hypothetical data (Section IV). Finally, we present the conclusions from this feasibility study and offer some recommendations. Some pertinent data are presented in the Appendix.

II. TLRS GROUND-TO-GROUND RANGING

Advantages and Problems

The TLRS is a highly mobile satellite laser ranging system designed to perform ground-to-LAGEOS range measurements. It is also highly sensitive, being capable of determining the range to a LAGEOS satellite with return signals as low as one photoelectron every 20 to 50 laser shots [Silverberg et al. 1982]. Used as a ground-to-ground ranging device, it can measure the distance to any single 1 inch (25 mm) corner reflector within sight at very low laser power level. The measureable range is limited only by the curvature of the earth. The required power level is so low that, unlike some systems used for similar measurements, the laser beam can be maintained many orders of magnitude below the eye-damage threshold.

The practical precision of the TLRS range measurements is limited to about 1.5 cm for a one minute average, which is somewhat worse than those of conventional EDM devices using modulated laser beams. However, the long range capability of the TLRS reduces the relative error to well within the limits of interest in conventional surveys. The TLRS has an automatic pointing system, an automatic calibration system and other features which lend themselves to providing many horizontal (ground-to-ground) line measurements on an operational basis. Thus it will be a good device to use if the data it provides is sufficient to determine the regional deformation at a high-enough accuracy.

The most serious problem in using the TLRS for ground-to-ground ranging is the atmospheric effect. The temperature, pressure, and to a lesser degree water vapor influence the index of refraction of air, and thus the speed of a laser beam through the atmosphere. To obtain the absolute distance between two points from a time of flight measurement through air, one must make corrections for these atmospheric variables.

Estimates of these atmospheric variables along the beam path may be made based on measurements at the two end points. This, however, is unsatisfactory for long lines. A more precise way is to measure directly the atmospheric condition along the beam path by flying an aircraft during the ranging. This, though done in practice, is a costly operation. A third alternative is to use more than one wavelength for ranging. Using the dispersive characteristics of light in air, one can correct for the atmospheric effects [Huggett, et al. 1977].

The present TLRS operates in a single color. Flying an aircraft, we judged, is too costly for repeated measurements in many directions. Thus we had to look for another alternative.

Relative Lateration

One way to improve the accuracy of range measurements without relying on expensive in-flight measurement of atmospheric conditions is to use a relative lateration technique, or the "ratio method" (Robertson, 1972). Instead of attempting to measure the absolute length of each survey line to high accuracy, this technique determines only the ratios of distances. This method is based on a supposition that the temporal changes of atmospheric conditions along several survey lines within a given region are similar to each other. Therefore, even when the time of flight of a laser beam in each line fluctuates with changing atmospheric conditions, the ratios of the times of flight along different survey lines tend to vary little with time.

Carter and Vincenty [1978] used this method in an experimental EDM survey around the McDonald Observatory in 1977. They obtained sets of measurements, one month apart, consistent to one to two parts in 10^7 . They have just repeated this experiment and the data is now being analyzed. Since the results of Carter and Vincenty appear to be quite promising, we have decided to try the same for our TLRS measurements.

Relationship Between Relative Lateration and Strain

Unlike absolute measurements of distances, the relative distance measurements repeated after a certain time period will not give all of the components of deformation, or incremental strain, for the time period unless at least one survey line is measured absolutely. However, a clear relationship exists between the changes of relative distances and incremental shear strain.

Let us consider n survey lines radiating from a central station. In the present case, the TLRS is located at the central station and a retroreflector is located at the end of each radiating line. Assume that all lines lie in a horizontal plane, neglecting both the curvature of the earth's surface and topographic height differences. Choosing a coordinate system with the origin at the central station, positive x towards east and positive y towards north, the original length of line i to the reflector at coordinates (x_i, y_i) at the time of the initial survey is given by

$$s_i = (x_i^2 + y_i^2)^{1/2} \quad (1)$$

Now assume that between the initial survey and a subsequent survey the entire area of the survey undergoes a uniform deformation represented by incremental strain components ϵ_{xx} , ϵ_{xy} and ϵ_{yy} . Then, the line length becomes

$$\begin{aligned}
 s_i' &= [(x_i + \epsilon_{xx}x_i + \epsilon_{xy}y_i)^2 + (y_i + \epsilon_{xy}x_i + \epsilon_{yy}y_i)^2]^{1/2} \\
 &= [x_i^2 + y_i^2 + 2\epsilon_{xx}x_i^2 + 4\epsilon_{xy}x_iy_i + 2\epsilon_{yy}y_i^2]^{1/2} \\
 &= s_i [1 + 2\epsilon_{xx}\sin^2\alpha_i + 4\epsilon_{xy}\sin\alpha_i\cos\alpha_i + 2\epsilon_{yy}\cos^2\alpha_i]^{1/2} \\
 &= s_i [1 + \epsilon_{xx}\sin^2\alpha_i + \epsilon_{xy}\sin 2\alpha_i + \epsilon_{yy}\cos^2\alpha_i] \quad (2)
 \end{aligned}$$

where $\alpha_i = \tan^{-1}(x_i/y_i)$ is the azimuth of the line i measured clockwise from north, and the higher order terms in strain have been neglected. Then, the range increment δ_i is given by

$$\delta_i = s_i' - s_i = s_i [\epsilon_{xx}\sin^2\alpha_i + \epsilon_{xy}\sin 2\alpha_i + \epsilon_{yy}\cos^2\alpha_i] \quad (3)$$

Next define original mean range and range ratios to the mean, respectively, as

$$\bar{s} = \frac{\sum_{i=1}^n s_i}{n} \quad (4)$$

and

$$r_i = s_i/\bar{s} \quad (5)$$

Then, the subsequent mean range and range ratios are

$$\bar{s}' = \frac{\sum_{i=1}^n s_i'}{n} = \bar{s} + \frac{\sum_{i=1}^n \delta_i}{n} \quad (6)$$

and

$$\begin{aligned}
 r_i' &= s_i'/\bar{s}' = (s_i + \delta_i)/(\bar{s} + \frac{\sum_{i=1}^n \delta_i}{n}) \\
 &= r_i (1 + \delta_i/s_i - \frac{\sum_{i=1}^n \delta_i}{n\bar{s}}) \quad (7)
 \end{aligned}$$

where the higher order terms are again neglected. The increment of the range ratio is, therefore,

$$r_i' - r_i = r_i (\delta_i/s_i - \frac{\sum_{i=1}^n \delta_i}{n\bar{s}}) \quad (8)$$

Then, range ratio increment normalized by the original range ratio is given by

$$\gamma_i = (r_i' - r_i)/r_i = \delta_i/s_i - \frac{1}{n} \sum_{i=1}^n \delta_i / \bar{ns} \quad (9)$$

Substituting eq. (3) into eq. (9), and using (5), we obtain

$$\begin{aligned} \gamma_i = & [\sin^2 \alpha_i - \frac{1}{n} \sum_{i=1}^n (r_i \sin^2 \alpha_i) / n] \epsilon_{yy} \\ & + [\sin 2\alpha_i - \frac{1}{n} \sum_{i=1}^n (r_i \sin 2\alpha_i) / n] \epsilon_{xy} \\ & + [\cos^2 \alpha_i - \frac{1}{n} \sum_{i=1}^n (r_i \cos^2 \alpha_i) / n] \epsilon_{yy} \end{aligned} \quad (10)$$

Equation (10) may give one an impression that a set of measurements of the normalized range ratio increments γ_i would give the incremental strain components ϵ_{xx} , ϵ_{xy} and ϵ_{yy} . However, this impression is incorrect because the coefficients of ϵ_{xx} and ϵ_{yy} are not independent of each other, as their sum vanishes, and therefore ϵ_{xx} and ϵ_{yy} cannot be determined uniquely.

Now let

$$\Theta = \epsilon_{xx} + \epsilon_{yy} \quad (11)$$

and

$$\Psi = \epsilon_{xx} - \epsilon_{yy} \quad (12)$$

Then,

$$\epsilon_{xx} = \frac{1}{2} (\Theta + \Psi) \quad (13)$$

and

$$\epsilon_{yy} = \frac{1}{2} (\Theta - \Psi) \quad (14)$$

Substituting (13) and (14) into (10), we obtain

$$\begin{aligned} \gamma_i = & [\sin 2\alpha_i - \frac{1}{n} \sum_{i=1}^n (r_i \sin 2\alpha_i) / n] \epsilon_{xy} \\ & - \frac{1}{2} [\cos 2\alpha_i - \frac{1}{n} \sum_{i=1}^n (r_i \cos 2\alpha_i) / n] \Psi \end{aligned} \quad (15)$$

The coefficients of ϵ_{xy} and Ψ are known quantities for the initial setup of the survey lines. Thus, for a set of measurements of the normalized range ratio increments γ_i , the incremental shear strain components ϵ_{xy} and Ψ can be determined by a least-square inversion of eq. (15).

Finally, the maximum incremental shear strain S and the direction of the principal strain axes β are given by

$$S = [(2\epsilon_{xy})^2 + \Psi^2]^{1/2} \quad (16)$$

and

$$\beta = \frac{1}{2} \tan^{-1} (2\epsilon_{xy} / \Psi) \quad (17)$$

The dilation Θ of eq. (11) disappears from eq. (15), and thus cannot be determined. This is expected because any uniform compression or expansion of the entire area causes no change in range ratios.

The treatment above assumes uniform deformation of the entire region. If for some reason, such as the existence of active faults within the area, the regional deformation is not uniform, large residuals will show up in the least-square inversion of eq. (15). Thus, any residuals significantly larger than the measurement errors will indicate heterogeneous strain.

The remaining question is how accurately we can estimate the normalized range ratio increments γ_i . Since the measurements are done in terms of time of flight of light beams, the uncertainty in speed of light is the determining factor. The average speed of light, c_i , between the central station and a reflector i may be expressed as the sum of four components:

$$c_i = c_0 + \ell_i + w_c + w_i \quad (18)$$

where c_0 is the speed of light in standard air, which is constant for all survey lines at all times; ℓ_i is the correction attributable to the reflector location, which is time invariant for a given reflector; w_c is a component of correction attributable to weather common to all reflectors at a given time; and w_i is the residual weather correction. The line length s_i is given in terms of round-trip time of flight, t_i , as

$$s_i = \frac{1}{2}(c_0 + \ell_i + w_c + w_i)t_i \quad (19)$$

the mean range as

$$\bar{s} = \frac{1}{2}(c_0 \bar{t} + \sum_{i=1}^n \ell_i t_i / n + w_c \bar{t} + \sum_{i=1}^n w_i t_i / n) \quad (20)$$

where $\bar{t} = \sum_{i=1}^n t_i / n$ is the mean time of flight, and the range ratio to the mean as

$$r_i = u_i [1 + (\ell_i - \sum_{i=1}^n \ell_i t_i / n \bar{t} + w_i - \sum_{i=1}^n w_i t_i / n \bar{t}) / c_0] \quad (21)$$

where $u_i = t_i / \bar{t}$ is the time-of-flight ratio to the mean, and the higher-order terms have been neglected. Finally, the normalized range ratio increment is given as

$$\gamma_i = \eta_i + [(w_i' - w_i) - \sum_{i=1}^n (w_i' - w_i) t_i / n \bar{t}] / c_0 \quad (22)$$

where $\eta_i = (u_i' - u_i)/u_i$ is the normalized time-of-flight ratio increment and quantities with primes designate those at subsequent measurement as before. The higher-order terms are again neglected. Note that the common weather component, w_c , is eliminated by taking the range ratio (21), and the location specific components, w_i 's, are eliminated by normalization (22), leaving only the residual weather components w_i 's.

The normalized time-of-flight ratio increment, η_i , thus approximates the range ratio increments, γ_i , with a small error due to residual weather term. The latter is not location specific, and is not common to all lines at a given time. If this term is sufficiently small, then we can substitute η_i for γ_i in calculating the shear strain increment using (15).

III. MT. WILSON EXPERIMENT

Field Experiment

At the request of the NASA Crustal Dynamics Project, the TLRS team from the McDonald Observatory of the University of Texas, led by Dr. Eric Silverberg, deployed the TLRS at Mt. Wilson, California, in January of 1981. At the same time, two of us (H.J.D. and T.C.) scouted the surrounding area for suitable target sites and selected the reflector locations. Then, a field party from the National Geodetic Survey (NGS), which was dispatched at the request of NASA to help us, deployed retroreflectors at the chosen sites. The survey lines selected for the site are shown in Figure 1. Table 1 lists the nominal coordinates of the base station (TLRS site) at Mt. Wilson and of the end points of the lines, where the retroreflectors were installed. Also listed in Table 1 are the approximate look angles from Mt. Wilson and ranges as computed from the indicated coordinates using the IAG standard ellipsoid Geodetic Reference System 1967.

Each reflector except the one at Cahuenga was a metal box containing an array of three 1½ inch (38mm) corner cubes, supplied by the NGS. The box was mounted on a tripod and placed directly over the station mark using an optical blumb bob. This elaborate configuration made it necessary to guard the reflector continuously for the entire duration of the experiment. The reflector used at Cahuenga was designed by one of us (T.C.) for unmanned operation. It contained a single 1 inch (25mm) corner cube and was fastened to an outcrop with anchor bolts at a site off the station mark, thus concealed from public view.

The reference point of the TLRS, from which the raw time-of-flight measurements were made, was slightly offset from the Mt. Wilson station mark given in Table 1. The measured coordinates of the station mark relative to the TLRS were:

$$x = -1.4873 \text{ m (west)}$$

$$y = 0.5093 \text{ m (north)}$$

$$z = -3.3709 \text{ m (below)}$$

The resulting corrections, to be applied to the observed quantities to reduce them to the reference mark, are listed in Table 2. The corrections can be applied at any stage of data reduction.

After the initial setup, which began on January 9, 1981, the horizontal ranging data were collected over the four-day interval January 23 through 26, 1981, in cooperation with the NOAA National Geodetic Survey. Each of the reflector sites except Cahuenga was manned continuously during the entire experiment to record the temperature, pressure and relative humidity at the site at about 30 minute intervals. The details of the data acquisition are given in Silverberg et al. [1982].

1981 MT. WILSON
RADIAL LINE SURVEY

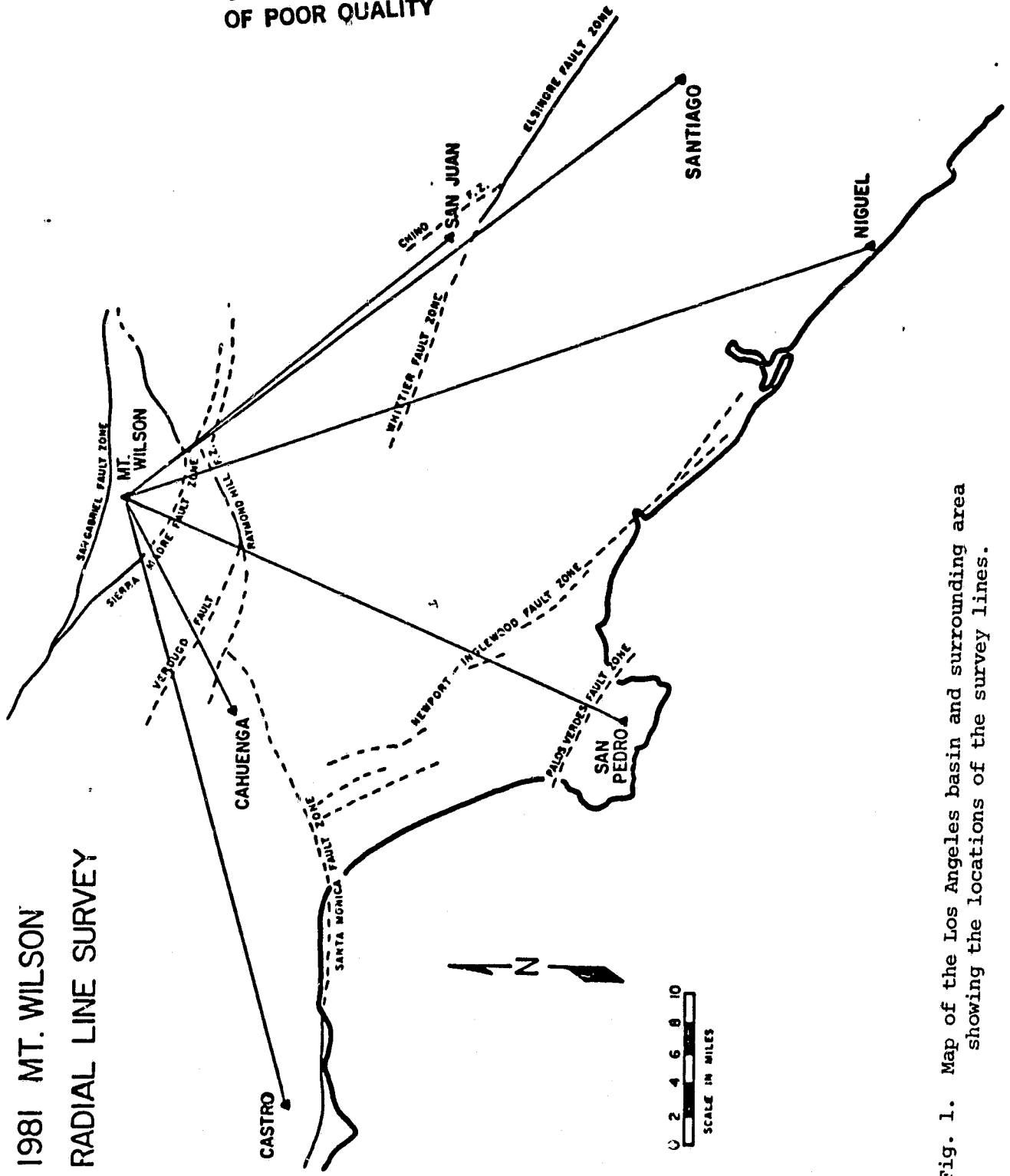


Fig. 1. Map of the Los Angeles basin and surrounding area showing the locations of the survey lines.

ORIGINAL PAGE IS
OF POOR QUALITY

Table 1. Stations Used in Mt. Wilson Line Survey

Station	Longitude	Latitude	Elevation m	Look Angle		Range m	Note
				Azimuth	Altitude		
Mt. Wilson	241° 56' 17.85"	34° 13' 21.58"	1722.0				1
Castro	241° 12' 55.40"	34° 05' 08.57"	858.9	257.366	-1.030	68393	2
Cahuenga	241° 40' 29.81"	34° 08' 13.00"	554.1	249.687	-2.681	26104	3
San Pedro	241° 39' 55.73"	33° 44' 40.88"	447.1	205.506	-1.508	58729	4
Niguel	242° 16' 00.18"	33° 30' 44.83"	288.0	158.814	-1.353	84459	
Santiago	242° 28' 00.10"	33° 42' 37.89"	1733.0	139.168	-0.329	74933	
San Juan	242° 15' 45.99"	33° 54' 49.47"	543.0	138.751	-1.688	45536	

- 1 New marker 9.408m from Mt. Wilson E10A @345° 17'
 2 Solitice Canyon B2 Aux. 1, which is 14.107m FNE of Castro 1898
 3 Reference mark #3 of Cahuenga #2, 13.329m @257° 47' from Cahuenga #2
 4 L7 Ecc. San Pedro Hills, which is 12.576m @318° 57' from San Pedro #3

Table 2. Corrections to be Applied to Observations to Reduce to Mt. Wilson Ground Marker

Station	Round-Trip	Range m	Range Ratio*	
	Time of Flight ns		(1)	(2)
ppm				
Castro	-9.344	-1.4003	-25.08	-26.78
Cahuenga	-9.054	-1.3568	-23.35	-23.51
San Pedro	-1.798	-0.2694	-5.91	-7.93
Niguel	6.222	0.9325	13.61	9.93
Santiago	8.931	1.3385	20.64	17.07
San Juan	8.432	1.2636	20.89	17.64

- * (1) Ratio to mean range
 (2) Same but excluding Cahuenga and Niguel

The Data

The raw field data were initially processed at the University of Texas at Austin by the McDonald Observatory group. As described in detail by Silverberg *et al.* [1982], the processing of the raw data involved accumulation of individual photon returns into 200 psec bins, smoothing of the coadded returns by three-bin (600 psec) running averages, cross-correlation with a reference standard to eliminate long-term drift in the calibration constants, adjustments to account for certain measurement irregularities, and removal of a 86.8 nsec constant calibration correction.

The calibrated round-trip time-of-flight data, shown in Figure 2 and listed in Table A1 in the Appendix, have not been corrected for the offset of the TLRS from the ground marker (Table 2). The data for Cahuenga were not used for the analysis because of certain processing difficulties encountered for the data for this station.

The data gap during the second day of observation was due to an interruption in data acquisition caused by rain which accompanied the passage of a cold front. The meteorological data taken at Mt. Wilson site and other stations are shown in Figures A1 through A3, and are listed in Table A2 in the Appendix.

As expected, the raw time-of-flight data show large fluctuations, which are only partially correlated with the meteorological data. The relative RMS deviations of the time-of-flight data (Table 3, column 3) range from 1.53 ppm for Niguel, which was surveyed only after the passage of the cold front, to 3.78 ppm for San Juan, which was the shortest line. The weighted average for all lines is 2.84 ppm.

Range Ratios to a Single Reference Line

Silverberg *et al.* [1982] calculated the time-of-flight ratios and atmosphere-corrected range ratios to a reference line following the procedure used by Carter and Vincenty [1978]. The reference line they chose was a smoothed curve (a cubic spline) through the Santiago data. Their results (Table 3, column 5) show relative RMS deviations of time-of-flight ratios ranging from 0.4 ppm for Niguel to 1.6 ppm for San Juan. The weighted average for all lines is 1.0 ppm, which is about a factor of three improvement from the fluctuation of the time-of-flight data.

Their results for the range ratios with atmospheric corrections based on end-point meteorological data did not fare as well. In fact the relative RMS deviations increased typically about 40% from those of uncorrected time-of-flight ratios [Silverberg *et al.* 1982].

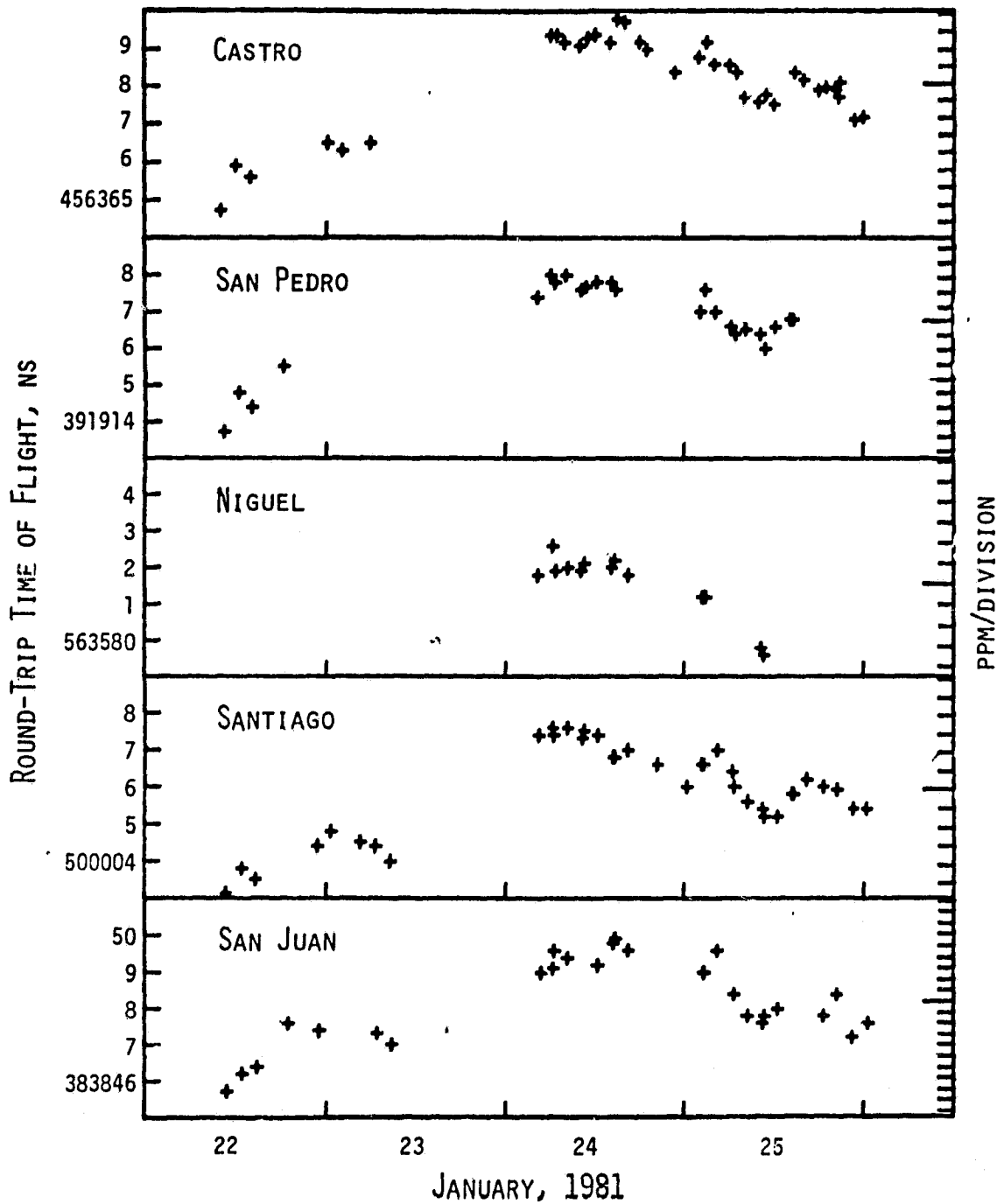


Fig. 2. Round-trip time of flight from Mt. Wilson. The data are not corrected for the marker offset.

The main reason for the poor performance of atmosphere-corrected values is the difficulty of making proper atmospheric corrections. A comparison of the variations of the group index of refraction calculated from the temperature and pressure at end points (Figure 3; also listed in Table A3 in the Appendix) with the time-of-flight variations (Figure 2) clearly shows that long-term variations are fairly well matched but shorter diurnal fluctuations are larger for the index of refractions than for the times-of-flight. Thus the index-of-refraction correction per Carter and Vincenty [1978] over-compensates for diurnal variations.

Time-of-Flight Ratios to the Mean

In order to be consistent with the range-ratio/strain relationship of the preceding section, we calculated the time-of-flight ratios to the mean. Since the time-of-flight measurements to all targets were not made exactly simultaneously, the data were linearly interpolated before the mean time-of-flight for a given time was calculated. (Higher order interpolations or a spline approximation might be better, but we judged the difference would be small.) Also, since we had data for Niguel only during the last half of the experiment, this station was excluded from the mean time-of-flight calculation.

The resulting time-of-flight ratios to the mean (Figure 4; also listed in Table A4 in the Appendix) show a further improvement in the fluctuations of the results. The relative RMS deviations (Table 3, column 5) now range from 0.36 ppm for Niguel to 1.24 ppm for San Juan, with the weighted average of 0.71 ppm for all lines, a factor of four improvement from the raw time-of-flight data.

An Alternative Atmospheric Correction

As stated earlier, the short-term, diurnal fluctuations in the index of refraction at end points exceed the observed fluctuations in the time-of-flight values. This is probably due to the larger fluctuation of the atmospheric temperature near the ground than those in most of the intervening air mass; a result of the base station and most of the target stations being located well above the intervening terrain. In this situation, a standard correction procedure like that of Carter and Vincenty [1978] is not really applicable, and some alternate procedures are needed.

An experimental procedure we tried was to estimate the average temperature of the air mass by low-pass filtering the mean of the temperatures measured at the end points. The filter we used was a simple one of adding all previous temperature readings each weighted by a factor proportional to a negative exponential of the elapsed time. After

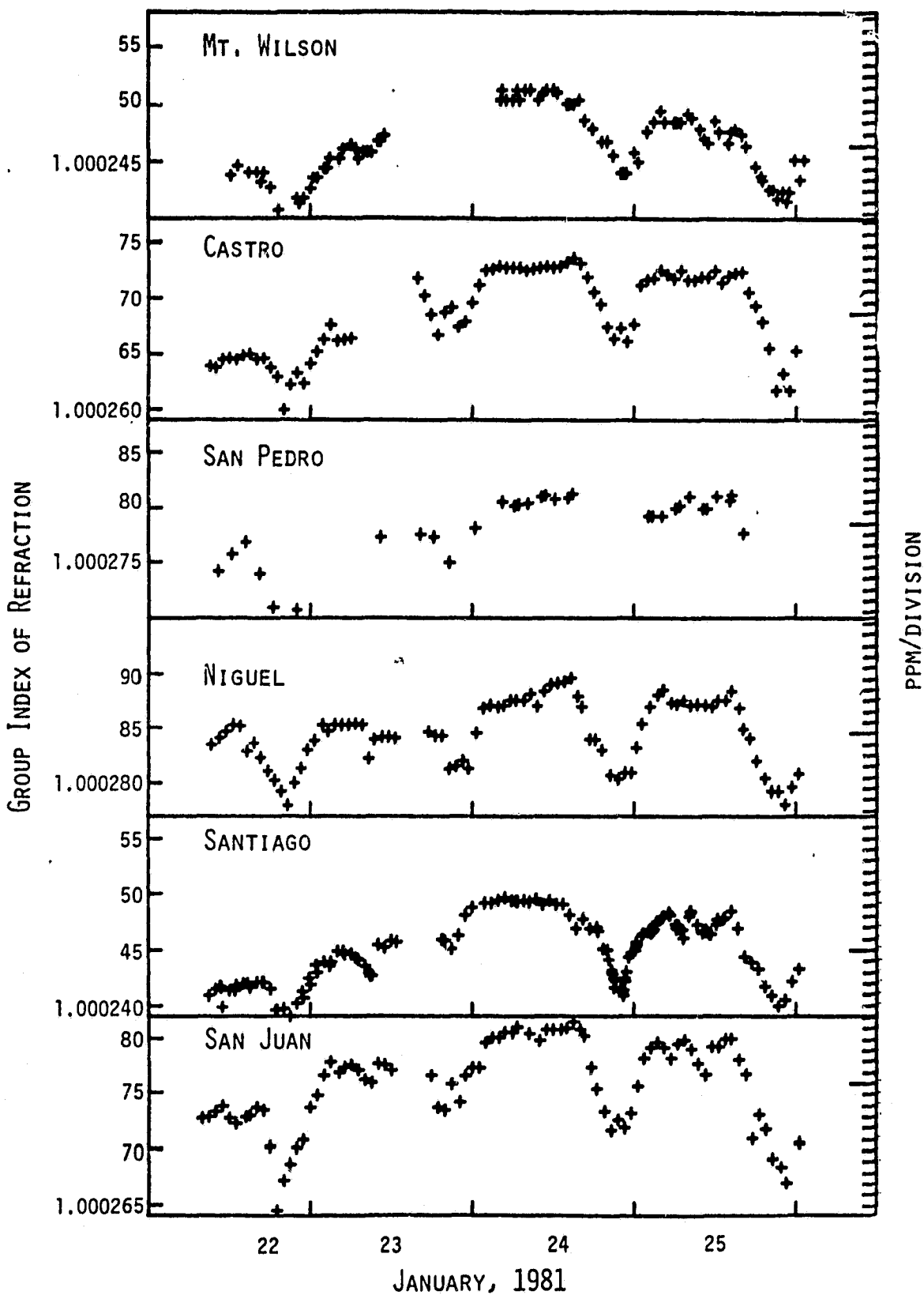


Fig. 3. Group index of refraction computed from atmospheric data at end points.

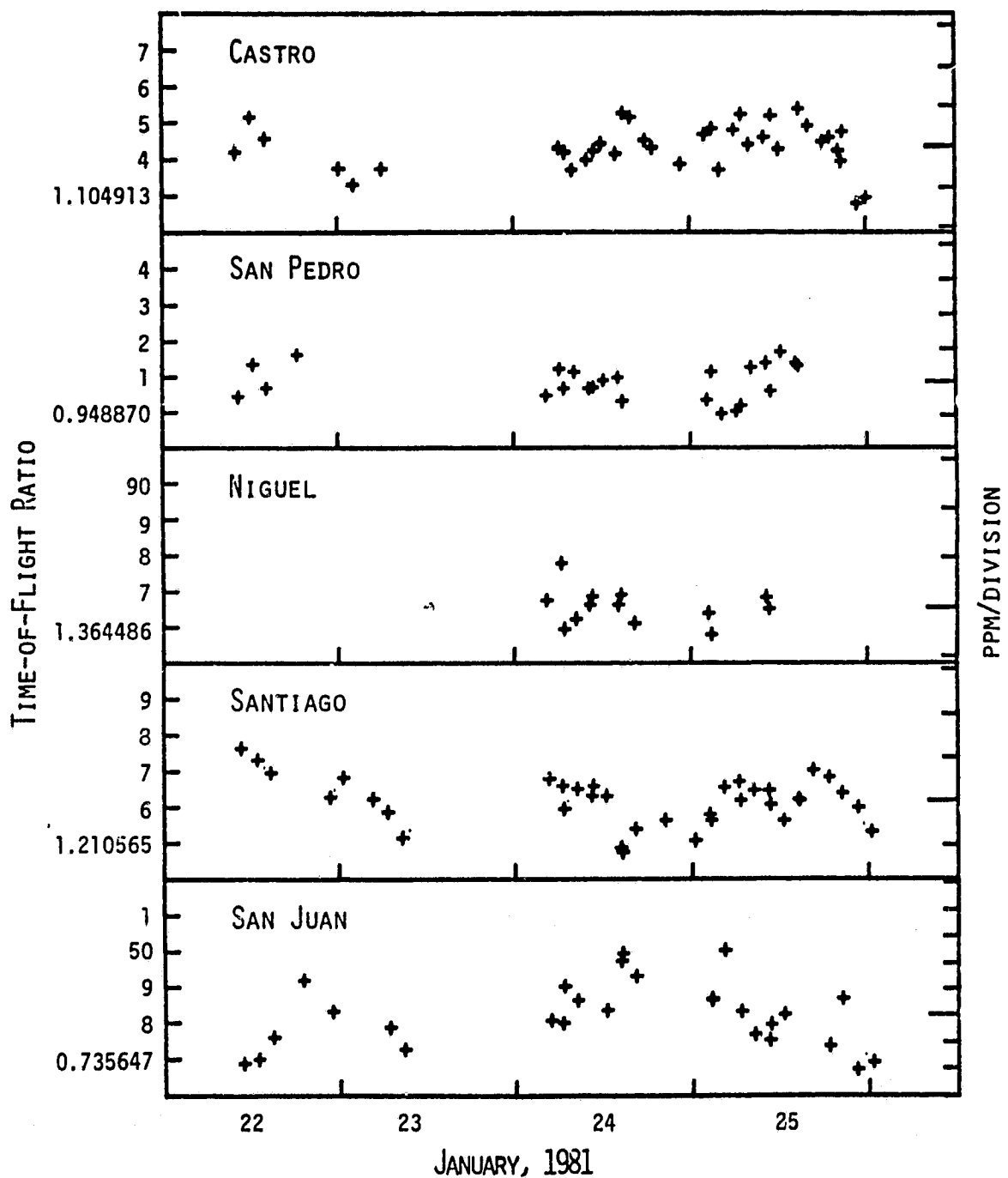


Fig. 4. Time-of-flight ratios to the mean.

trials with such filters of several different time constants, a time constant of 12 hours was found to give the best result. The resulting relative RMS deviations of the ranges thus corrected for atmospheric conditions (Table 3, column 4) range from 0.96 ppm for Castro to 2.05 ppm for San Juan with the weighted average of 1.38 ppm for all lines. This is about a factor of two improvement from the raw time-of-flight data. However, the range ratios calculated from these corrected ranges do not show any significant improvement over those of the uncorrected ratios. The relative RMS deviations of the corrected range ratios (Table 3, last column) range from 0.52 ppm for Niguel and Santiago to 1.21 ppm for San Juan, with the weighted average of 0.72 ppm for all lines.

A comparison of the relative RMS deviations of various quantities in Table 3 reveals that the best result is obtained for the uncorrected time-of-flight ratios to the mean. The atmospheric corrections did not improve the RMS deviations at all when ratios were taken.

A Test for Systematic Error Due to Atmospheric Conditions

The reliability of the relative lateration depends on the validity of the assumption that the temporal changes of atmospheric conditions are similar for all survey lines in the area so that their effects cancel out when ratios are taken. If this assumption is incorrect, a systematic error due to varying atmospheric conditions is introduced into the measured time-of-flight ratios. The greatly different atmospheric conditions before and after the passage of a cold front during the experiment gave us an opportunity to test this assumption.

The test we performed is the likelihood ratio test. We divided the time-of-flight ratios of Table A4 for each line into two subsets, the first half and the last half, of equal size (the last half was one greater than the first half if the total number was odd). If the systematic error due to atmospheric conditions is significantly large, the mean ratio, μ_1 , for the first subset will be significantly different from that, μ_2 , for the second subset. Setting up a null hypothesis $H_0: \mu_1 = \mu_2$, if it is true, then the likelihood ratio statistic

$$t = [n_1 n_2 / (n_1 + n_2)]^{1/2} (\mu_1 - \mu_2) / [(n_1 \sigma_1^2 + n_2 \sigma_2^2) / (n_1 + n_2 - 2)]^{1/2} \quad (23)$$

has a t distribution with $n_1 + n_2 - 2$ degrees of freedom, where n_1 and n_2 are the sample sizes of the two subsets and μ_1, μ_2, σ_1^2 and σ_2^2 are used to designate the sample means and the sample variances of the first and the second subsets, respectively, for convenience.

At 90% significance level, the t distribution has values of 1.69 for 34 degrees of freedom and 1.80 for 11 degrees of freedom, while the t values computed from the data, Table 4, are much smaller. Therefore, the null hypothesis cannot be rejected at this level of significance.

ORIGINAL PAGE 19
OF POOR QUALITY

Table 3. Comparison of Relative RMS Deviations in ppm

Station	Number of Data Points	Uncorrected Time of Flight	Corrected Range(a)	Uncorrected T-o-F Ratio to Santiago(b)	Uncorrected T-o-F Ratio to the mean	Corrected Range Ratio to the mean
Castro	36	2.68	0.96	0.7	0.56	0.54
San Pedro	24	2.91	1.12	0.8	0.52	0.54
Niguel	13	1.53	1.81	0.4	0.36	0.52
Santiago	36	2.45	1.03	(0.2)	0.54	0.52
San Juan	27	3.78	2.05	1.6	1.24	1.21
All	136	2.84	1.38	1.0	0.71	0.72

(a) Corrected by using 12-hour low-pass filtered temperature

(b) From Silverberg et al. [1982]. The deviation for Santiago is from the smoothed curve, and is not included in calculating the average for all stations.

Table 4. Likelihood Ratio Test for Non-equality of Means

Station	Subset 1			Subset 2			Degree of Freedom	t
	n_1	μ_1	σ_1	n_2	μ_2	σ_2		
Castro	18	1.104914282	0.000000513	18	1.104914438	0.000000694	34	0.745
San Pedro	12	0.948870911	0.000000356	12	0.948870818	0.000000598	22	0.445
Niguel	6	1.364486713	0.000000572	7	1.364486460	0.000000365	11	0.889
Santiago	18	1.210566249	0.000000774	18	1.210566130	0.000000515	34	0.531
San Juan	13	0.735648159	0.000000830	14	0.735648288	0.000000983	25	0.353

In other words, no significant difference is found between the mean time-of-flight ratios in the first and second halves of the experiment for any of the lines surveyed.

Results

Since there is no evidence for systematic errors caused by atmospheric conditions, the most likely estimates of the mean time-of-flight ratios and their variances (and standard deviations) can be calculated from the entire data set. The results are shown in Table 5. Also listed in this table are the mean time-of-flight and the mean distances. The latter were calculated using atmospheric corrections based on the low-pass filtered temperatures described earlier and pressures interpolated to the average height of the beam from the end-point measurements (extrapolation in case of Santiago because the average height of the beam was lower than either end point). A group index of refraction of $n_g = 1.00028975$ at the wavelength of $0.5320 \mu\text{m}$, calculated from the formula⁹ given in American Institute of Physics Handbook [1972, p. 6-111] for standard dry air with 0.03% carbon dioxide at 15°C and 760 mm Hg, is used. No other corrections have been applied to the calculated distances; thus they are subject to minor systematic errors.

The estimated relative standard deviations of the mean time-of-flight ratios are approximately 1×10^{-7} except for San Juan, which is the shortest line. In comparison, Savage and Prescott [1973] estimate that the standard deviation of their Geodolite measurements of distances are 3 and 8 mm for lengths of 1 and 37 km, respectively. Thus, the precision of the present time-of-flight ratios is at least a factor of two better than that of their distance measurements. Furthermore, their distances had to be corrected for temperature and humidity readings made with an aircraft flying along the line of sight, while the present time-of-flight ratios required no atmospheric correction at all.

Multiwavelength measurements of distances are definitely better than the above two in terms of relative accuracy. Huggett and Slater [1975] and Slater and Huggett [1976] show the standard deviation of individual distance measurements to be less than 1×10^{-7} on a 10.1 km line. By taking the mean of many measurements, which is practical in this case, the accuracy can be improved further. The ranges attainable with the multiwavelength system, however, are quite limited compared with the TLRS measurements.

ORIGINAL PAGE IS
OF POOR QUALITY

Table 5. Mean Time of Flight, Distance and Ratios*

Station	Mean Time of Flight ns	Mean Distance m	Mean T-o-F Ratio	S.D. of Mean T-o-F Ratio	Relative S.D. ppm
Castro	456358.75	68388.52	1.10488758	0.00000010	0.09
San Pedro	391914.94	58730.88	0.94886293	0.00000010	0.11
Niguel	563587.77	84456.72	1.36449651	0.00000014	0.10
Santiago	500014.83	74931.62	1.21058326	0.00000011	0.09
San Juan	303856.63	45535.87	0.77566587	0.00000018	0.24

* These results have been corrected for the TLRs/ground-marker offset.

Table 6. Increment in Normalized Ratio
Due to Hypothetical Strain Increment
and Rounded Values for Testing

Station	Normalized Ratio Increment ppm	Rounded to 0.1 ppm
Castro	0.052	0.1
San Pedro	-0.158	-0.2
Niguel	-0.030	0.0
Santiago	0.068	0.1
San Juan	0.070	0.1

IV. SHEAR STRAIN DETERMINATION USING HYPOTHETICAL DATA

We have been unable to reoccupy the Mt. Wilson site for a repeat measurement, which would allow a testing of the ratio method for a shear strain determination in the region. This section, therefore, describes an exercise we have conducted to see how well we can determine the regional shear-strain increment using a set of hypothetical data.

We assume a hypothetical strain increment described by

$$\begin{aligned} \epsilon_1 &= 0.1 \times 10^{-6} & : & \text{maximum extension} \\ \epsilon_2 &= -0.2 \times 10^{-6} & : & \text{maximum compression} \\ \epsilon_1 - \epsilon_2 &= 0.3 \times 10^{-6} & : & \text{maximum shear} \\ \beta &= 110^\circ & : & \text{azimuth of maximum positive principal} \\ & & & \text{axis (extension) measured clockwise} \\ & & & \text{from north} \end{aligned}$$

This strain increment is approximately the annual strain increment in southern California observed by Savage et al. [1981]. The resulting increments in normalized range ratios for the five survey lines used in the Mt. Wilson experiment are listed in the center column of Table 6. Since we will not be able to measure these ratio increments at this accuracy, we use the values rounded to 1×10^{-7} , as given in the rightmost column of Table 6.

Substituting these rounded ratio increments into eq. (15), and inverting it in a least-squares sense, we obtain the following results:

$$\begin{aligned} \epsilon_1 - \epsilon_2 &= 0.40 \times 10^{-6} \\ \beta &= 109.5^\circ \end{aligned}$$

The result describes the original hypothetical shear-strain increment reasonably well. A trial with a rounding to 1×10^{-8} results in almost complete duplication of the hypothetical strain increment.

The likelihood ratio test of the preceding section can be used to estimate the required number of measurements to achieve a given level of accuracy at a given confidence level. We use the standard deviation of individual range ratio measurements of 5×10^{-7} as estimated from the present data (Table 3, excluding San Juan). Thus, substituting $\sigma_1 = \sigma_2 = 10^{-6}$ and $|\mu_1 - \mu_2| = 10^{-7}$ into eq. (18), we find that $n_1 = n_2 = 200$ will give $t = 1.99$, which exceeds the value of t distribution, 1.97, for 198 degrees of freedom at 95% confidence level. Thus a variation in the range ratio of 10^{-7} found by averaging 200 ratio measurements is significant at 95% level of confidence.

At a rate of one measurement every hour, it will take slightly more than a week to complete this many measurements. Two such series of

measurements one year apart is sufficient to determine the shear strain increment in southern California.

For a given set of t and σ 's, n 's are approximately inversely proportional to the square of the difference in μ 's in equation (18). Thus doubling the measurement interval, thereby doubling the expected ratio variations, approximately quarters the required number of measurements. For example, a pair of 50-measurement sets two years apart will give the shear strain rate in southern California.

V. CONCLUSIONS AND RECOMMENDATIONS

Conclusions

Even though the field experiment we performed during this contract was quite limited compared with our original plan, we obtained several interesting and important results. The following is a list of conclusions drawn from these results:

1. The increment of the ratio of the length of a survey line to the average of several survey lines in a region is directly related to the incremental shear strain in the region. Thus, the shear strain rate can be calculated from observations of temporal variations in such ratios.
2. Using the TLRS, the time-of-flight ratios could be determined to an accuracy (one standard deviation) of 1×10^{-7} by averaging measurements over a four day period. This accuracy was obtained without using any atmospheric corrections at all. No improvement was obtained when atmospheric corrections based on end-point measurements were applied.
3. A calculation using a hypothetical data simulating the observed strain field in southern California indicates that two sets of TLRS ratio measurements separated by one to two years will be sufficient to determine the direction and rate of shear strain in the region.
4. Thus relative lateration using the TLRS has been demonstrated to be a good method for monitoring the regional shear strain field around satellite ranging stations. The TLRS operates successfully over long distances. The ratio method is extremely economical. It requires no environmental measurements and can be performed with small unattended retroreflectors distributed over a wide area. Thus these techniques greatly surpass the capability of conventional EDM techniques.

Recommendations

1. The results of the present experiment are thus very encouraging. However, they are based on only one experiment. Before this technique is put to a practical use, further demonstration is needed to confirm the above results. Therefore, it is recommended that this feasibility study be continued at least to include reoccupation of the Mt. Wilson site and two measurements at another properly selected site, preferably with a different meteorological environment.

2. Relative lateration is not limited to the data taken by the TLRS. The data reduction procedure used in the present study can be applied to other data from distance measurements. Therefore, it is recommended that we reanalyze some of existing ranging data to see if improvements in determination of shear strain rate can be achieved. This can be done without further field measurements.
3. Additional feasibility test measurements similar to the Mt. Wilson experiment may be obtained from fixed satellite ranging stations. It is therefore, recommended that this possibility be examined.
4. Horizontal ranging to distant targets on the ground does not require all the sophistication of the TLRS system. Therefore, when the capability of the present technique is fully demonstrated, a smaller, more portable single-photon ranging unit should be developed for this purpose.
5. Finally, the technology is advancing in other fields also. Such techniques as miniature interferometer terminals [Counselman and Shapiro, 1979] may someday be more useful in surveys of regional extent. Therefore, development in these other techniques should be reviewed while developing the present technique.

Acknowledgements

The initial data reduction of the Mt. Wilson experiment was done in the Astronomy Department of the University of Texas at Austin. We are grateful to Dr. Eric C. Silverberg for supplying us the processed data on a computer tape. Dr. Cliff Frohlich kindly reviewed a draft of this report, his constructive comments are greatly appreciated.

References

- American Institute of Physics Handbook, 3rd ed., McGraw-Hill, New York, 1972.
- Carter, W. E. and T. Vincenty, Survey of the McDonald Observatory radial line scheme by relative lateration technique, NOAA Technical Report NOS 74 NGS 9, 1978.
- Counselman III, C.C. and I.I. Shapiro, Miniature interferometer terminals for earth surveying, Bull. Geod. 53, 139-163, 1973.
- Huggett, G. R. and L. E. Slater, Precision electromagnetic distance-measuring instrument for determining secular strain and fault movement, Tectonophysics, 29, 19-27, 1975.
- Huggett, G. R., L. E. Slater and J. Langbein, Fault slip episodes near Hollister, California: Initial results using a multiwavelength distance-measuring instrument, J. Geophys. Res., 82, 3361-3368, 1977.
- Robertson, K. D., The use of line pairs in trilateration and traverse, Survey Rev., 21, 290-306, 1972.
- Savage, J. C. and W. H. Prescott, Precision of Geodolite distance measurements for determining fault movements, J. Geophys. Res., 78, 6001-6008, 1973.
- Savage, J. C., W. H. Prescott, M. Lisowski and N. E. King, Strain accumulation in southern California, 1973-1980, J. Geophys. Res., 86, 6991-7001, 1981.
- Silverberg, E. C., and D. L. Byrd, A mobile telescope for measuring continental drift, Sky and Telescope, 61, 405-408, 1981.
- Silverberg, E. C., T. Cahill and J. Dorman, Relative lateration across the Los Angeles basin using a satellite laser ranging system, Bull. Geod., (in press), 1982.
- Slater, L. E. and G. R. Huggett, A multiwavelength distance-measuring instrument for geophysical experiments, J. Geophys. Res., 81, 6299-6306, 1976.

APPENDIX

Table A1. Calibrated Round-Trip Time of Flight

Castro			San Pedro			Niguel			Santiago			San Juan												
dy	hr	mn	ns	dy	hr	mn	ns	dy	hr	mn	ns	dy	hr	mn	ns									
22	10	04	29	456364.7	22	10	18	55	391913.7	24	04	28	32	563581.8	22	10	41	41	500003.1	22	10	51	17	303845.7
22	12	02	41	456365.9	22	12	21	52	391914.8	24	06	19	58	563582.6	22	12	43	11	500003.8	22	12	51	51	303846.2
22	14	05	43	456365.6	22	14	15	03	391914.4	24	06	46	28	563581.9	22	14	34	32	500003.5	22	14	48	04	303846.4
23	00	09	40	456366.5	22	18	23	39	391915.5	24	08	18	26	563582.0	22	22	49	55	500004.4	22	18	55	03	303847.6
23	02	09	25	456366.3	24	04	20	40	391917.4	24	10	15	13	563581.9	23	00	41	06	500004.8	22	22	54	59	303847.4
23	06	05	03	456366.5	24	06	16	19	391918.0	24	10	40	16	563582.1	23	04	33	04	500004.5	23	06	47	01	303847.3
24	06	08	46	456369.4	24	06	51	04	391917.8	24	14	15	10	563582.0	23	06	39	34	500004.4	23	06	47	14	303847.0
24	06	58	17	456369.4	24	08	09	40	391918.0	24	14	40	18	563582.2	23	08	39	44	500004.4	24	04	40	14	303849.0
24	08	00	19	456369.2	24	10	10	03	391917.6	24	16	18	20	563581.8	24	04	40	08	500007.4	24	06	29	45	303849.1
24	08	59	54	456369.1	24	10	45	34	391917.7	24	16	18	20	563581.2	24	06	25	43	500007.6	24	06	35	37	303849.6
24	10	55	03	456369.3	24	12	10	04	391917.8	25	02	21	58	563581.2	24	06	41	31	500007.4	24	08	25	49	303849.4
24	12	00	58	456369.4	24	14	11	30	391917.8	25	02	48	49	563581.2	24	08	22	17	500007.6	24	12	25	08	303849.2
24	14	01	34	456369.2	24	14	45	60	391917.6	25	10	16	05	563579.8	24	10	21	13	500007.3	24	14	25	20	303849.8
24	14	55	05	456369.8	25	02	13	18	391917.0	25	10	41	13	563579.6	24	10	35	15	500007.5	24	14	35	04	303849.9
24	16	01	03	456369.7	25	02	53	27	391917.6	25	10	16	04	563581.2	24	12	20	03	500007.4	24	16	28	54	303849.6
24	18	00	06	456369.2	25	04	09	53	391917.0	25	10	16	04	563581.2	24	14	20	03	500006.8	25	02	33	03	303849.0
24	18	57	39	456369.0	25	06	10	05	391916.6	25	06	10	05	563581.2	24	14	35	11	563582.1	25	02	36	56	303849.6
24	22	44	42	456368.4	25	06	45	43	391916.4	25	06	45	43	563581.2	24	16	29	53	500007.0	25	04	25	60	303849.6
25	02	05	25	456368.8	25	08	11	36	391916.5	25	06	10	05	563581.2	24	16	29	53	500007.0	25	06	32	42	303849.4
25	02	58	04	456368.2	25	10	10	16	391916.4	25	08	11	36	563581.2	24	18	04	08	500006.6	25	08	25	56	303947.8
25	04	00	52	456368.6	25	10	45	23	391916.0	25	08	11	36	563581.2	25	00	25	13	500006.0	25	10	25	11	303847.6
25	06	01	17	456368.6	25	12	10	30	391916.6	25	08	11	36	563581.2	25	02	29	30	500006.6	25	10	36	03	303847.0
25	06	55	21	456368.4	25	14	15	11	391916.8	25	08	11	36	563581.2	25	04	22	37	500007.0	25	12	25	03	303849.0
25	08	04	49	456367.7	25	14	40	42	391916.8	25	06	22	51	500006.4	25	06	22	51	500006.4	25	18	31	55	303847.0
25	10	01	53	456367.6	25	14	40	42	391916.8	25	06	22	51	500006.4	25	06	22	51	500006.4	25	18	31	55	303847.0
25	10	55	08	456367.8	25	14	40	42	391916.8	25	06	22	51	500006.4	25	06	22	51	500006.4	25	20	25	59	303847.2
25	12	04	05	456367.5	25	14	40	42	391916.8	25	06	22	51	500006.4	25	06	22	51	500006.4	25	20	25	59	303847.2
25	14	51	54	456368.4	25	14	40	42	391916.8	25	06	22	51	500006.4	25	06	22	51	500006.4	25	20	25	59	303847.2
25	16	00	28	456368.2	25	14	40	42	391916.8	25	06	22	51	500006.4	25	06	22	51	500006.4	25	20	25	59	303847.2
25	18	00	19	456367.9	25	14	40	42	391916.8	25	06	22	51	500006.4	25	06	22	51	500006.4	25	20	25	59	303847.2
25	18	59	43	456368.0	25	14	40	42	391916.8	25	06	22	51	500006.4	25	06	22	51	500006.4	25	20	25	59	303847.2
25	20	07	42	456367.9	25	14	40	42	391916.8	25	06	22	51	500006.4	25	06	22	51	500006.4	25	20	25	59	303847.2
25	20	37	24	456367.7	25	14	40	42	391916.8	25	06	22	51	500006.4	25	06	22	51	500006.4	25	20	25	59	303847.2
25	20	49	58	456368.1	25	14	40	42	391916.8	25	06	22	51	500006.4	25	06	22	51	500006.4	25	20	25	59	303847.2
25	22	51	57	456367.1	25	14	40	42	391916.8	25	06	22	51	500006.4	25	06	22	51	500006.4	25	20	25	59	303847.2
26	00	05	27	456367.2	25	14	40	42	391916.8	25	06	22	51	500006.4	25	06	22	51	500006.4	25	20	25	59	303847.2

Table A2. (continued)

Time			T			P			V			Time			T			P			V					
dy	hr	mn	sc	deg	C	mmHg	mmHg	mmHg	dy	hr	mn	sc	deg	C	mmHg	mmHg	mmHg	dy	hr	mn	sc	deg	C	mmHg	mmHg	mmHg
24	09	00	00	6.1	693.1	6.2908	6.2908	719.3	22	12	20	00	13.4	719.3	9.2050	9.2050	740.3	22	19	33	00	16.1	740.3	11.8974	11.8974	
24	10	00	00	5.9	693.1	6.0500	6.0500	720.1	22	14	20	00	12.6	720.1	9.2050	9.2050	739.6	22	20	32	00	19.2	739.6	12.3337	12.3337	
24	11	00	00	5.8	693.1	5.8176	5.8176	720.1	22	16	20	00	15.6	720.1	9.9131	9.9131	736.8	22	21	40	00	16.7	736.8	13.2406	13.2406	
24	12	00	00	6.0	693.1	5.8176	5.8176	720.8	22	18	20	00	19.1	720.8	10.5698	10.5698	738.8	22	22	30	00	15.3	738.8	11.0974	11.0974	
24	13	00	00	5.8	693.1	5.8176	5.8176	719.3	22	22	00	00	18.7	719.3	11.8118	11.8118	739.6	22	23	37	00	13.9	739.6	11.4747	11.4747	
24	14	00	00	5.5	693.1	5.5931	5.5931	718.6	23	00	30	00	11.5	718.6	9.5532	9.5532	739.6	23	00	38	00	13.1	739.6	11.0653	11.0653	
24	15	00	00	5.1	693.1	5.5931	5.5931	720.8	23	16	30	00	12.1	720.8	10.2850	10.2850	739.6	23	01	45	00	11.6	739.6	11.0653	11.0653	
24	16	00	00	5.6	693.1	5.8176	5.8176	720.8	23	18	20	00	12.4	720.8	10.2850	10.2850	739.6	23	02	32	00	12.3	739.6	10.6688	10.6688	
24	17	00	00	6.8	693.1	6.5400	6.5400	720.8	23	20	30	00	14.7	720.8	11.8974	11.8974	739.6	23	03	35	00	11.6	739.6	10.2850	10.2850	
24	18	00	00	8.2	693.1	6.7978	6.7978	720.1	24	00	30	00	11.3	720.1	9.3777	9.3777	739.6	23	04	40	00	11.7	739.6	10.2850	10.2850	
24	19	00	00	9.3	693.1	7.2012	7.2012	720.8	24	04	20	00	9.1	720.8	8.6708	8.6708	739.6	23	05	30	00	11.6	739.6	10.2850	10.2850	
24	20	00	00	11.2	692.3	7.6258	7.6258	720.8	24	06	10	00	9.4	720.8	8.8679	8.8679	738.8	23	06	32	00	11.2	738.8	9.9131	9.9131	
24	21	00	00	12.0	691.6	7.6258	7.6258	720.8	24	06	45	00	9.3	720.8	8.7361	8.7361	738.8	23	07	30	00	11.3	738.8	9.9131	9.9131	
24	22	00	00	11.0	691.6	8.2263	8.2263	720.1	24	08	10	00	9.0	720.1	7.7721	7.7721	738.1	23	08	30	00	14.1	738.1	9.5532	9.5532	
24	23	00	00	12.0	690.8	8.2263	8.2263	720.1	24	10	10	00	8.3	720.1	8.2263	8.2263	738.8	23	09	29	00	12.7	738.8	10.6688	10.6688	
25	00	00	00	10.3	690.8	7.3403	7.3403	720.1	24	10	45	00	8.2	720.1	7.8610	7.8610	741.8	23	10	35	00	12.4	741.8	10.2850	10.2850	
25	01	00	00	6.6	690.8	6.0500	6.0500	720.1	24	12	10	00	8.6	720.1	7.7721	7.7721	741.8	23	11	30	00	12.4	741.8	10.2850	10.2850	
25	02	00	00	5.8	690.1	6.0500	6.0500	720.1	24	14	10	00	8.4	720.1	7.6258	7.6258	741.8	23	12	40	00	12.5	741.8	10.2850	10.2850	
25	03	00	00	5.7	690.1	6.5400	6.5400	720.1	24	14	45	00	8.1	720.1	7.6258	7.6258	741.8	23	17	40	00	13.1	741.8	11.4747	11.4747	
25	04	00	00	5.3	690.8	5.8176	5.8176	719.3	25	02	10	00	9.8	719.3	8.5418	8.5418	741.8	23	18	34	00	13.5	741.8	13.2486	13.2486	
25	05	00	00	5.7	690.8	5.3762	5.3762	719.3	25	02	52	00	9.8	719.3	8.7036	8.7036	741.8	23	19	30	00	13.5	741.8	11.0653	11.0653	
25	06	00	00	5.7	690.1	5.1669	5.1669	719.3	25	04	10	00	9.8	719.3	8.2263	8.2263	741.1	23	20	40	00	16.3	741.1	12.3337	12.3337	
25	07	00	00	5.0	690.1	5.3762	5.3762	720.1	25	06	10	00	9.4	720.1	6.7978	6.7978	741.1	23	21	33	00	15.0	741.1	11.4747	11.4747	
25	08	00	00	5.6	689.3	5.3762	5.3762	718.6	25	06	45	00	8.6	718.6	6.4143	6.4143	741.1	23	22	30	00	15.5	741.1	11.4747	11.4747	
25	09	00	00	5.5	689.3	5.3762	5.3762	718.6	25	08	10	00	8.8	718.6	6.0500	6.0500	741.1	23	23	26	00	16.2	741.1	11.0653	11.0653	
25	10	00	00	5.3	689.3	5.5931	5.5931	718.6	25	10	10	00	8.8	718.6	6.7978	6.7978	741.8	24	00	30	00	13.0	741.8	9.9131	9.9131	
25	11	00	00	4.7	689.3	5.3762	5.3762	718.6	25	10	45	00	8.8	718.6	6.7978	6.7978	741.8	24	01	40	00	11.0	741.8	9.2050	9.2050	
25	12	00	00	5.3	689.3	5.3762	5.3762	718.6	25	12	10	00	7.8	718.6	6.2908	6.2908	741.8	24	02	40	00	10.7	741.8	9.2050	9.2050	
25	13	00	00	5.5	688.6	5.8176	5.8176	717.8	25	14	10	00	7.8	717.8	7.0645	7.0645	741.8	24	03	50	00	10.8	741.8	9.2050	9.2050	
25	14	00	00	5.2	689.3	5.3762	5.3762	718.6	25	14	22	00	7.6	718.6	6.7978	6.7978	741.8	24	04	35	00	10.7	741.8	9.2050	9.2050	
25	15	00	00	5.3	690.1	5.5931	5.5931	719.3	25	16	10	00	11.4	719.3			741.8	24	05	40	00	10.3	741.8	9.2050	9.2050	
25	16	00	00	5.4	690.8	5.3762	5.3762		25	16	10	00					741.8	24	05	40	00	10.3	741.8	9.2050	9.2050	
25	17	00	00	7.3	690.8	5.9327	5.9327		24	05	20	00	10.3	741.8			741.8	24	06	20	00	10.3	741.8	9.8679	9.8679	
25	18	00	00	8.5	690.8	6.2908	6.2908		24	07	35	00	10.2	741.8			741.8	24	07	35	00	10.2	741.8	8.8679	8.8679	
25	19	00	00	10.0	690.8	6.6678	6.6678		24	08	35	00	9.7	741.8			741.8	24	08	35	00	9.7	741.8	8.5418	8.5418	
25	20	00	00	12.3	690.1	6.7978	6.7978		24	09	30	00	10.4	741.1	8.8679	8.8679	741.1	24	09	30	00	10.4	741.1	9.2650	9.2650	
25	21	00	00	16.2	689.3	8.2263	8.2263		24	10	30	00	9.2	741.1	9.2050	9.2050	741.1	24	10	30	00	9.2	741.1	8.5418	8.5418	
25	22	00	00	14.1	688.6	6.5400	6.5400		24	11	30	00	12.0	738.8	9.2050	9.2050	741.1	24	11	39	00	8.5	741.1	8.2263	8.2263	
25	23	00	00	16.1	689.3	7.3403	7.3403		24	12	30	00	11.4	738.8	9.2050	9.2050	741.1	24	12	31	00	8.4	741.1	9.2263	9.2263	
26	00	00	00	12.5	690.1	6.7978	6.7978		24	13	31	00	11.5	738.8	9.7318	9.7318	740.3	24	13	33	00	8.0	740.3	7.9210	7.9210	
									24	14	30	00	14.1	739.6	9.9131	9.9131	740.3	24	14	31	00	7.7	740.3	7.6258	7.6258	
									24	15	41	00	13.6	740.3	9.5532	9.5532	740.3	24	15	35	00	9.3	740.3	8.5418	8.5418	
									24	16	36	00	15.0	740.3	10.6688	10.6688	741.1	24	16	17	00	10.6	741.1	9.2050	9.2050	
									24	17	30	00	16.2	740.3	11.0653	11.0653	741.1	24	17	20	00	13.6	741.1	9.9131	9.9131	
22	10	21	00	14.7	718.6	9.9131	9.9131		24	18	31	00	17.1	740.3	12.3337	12.3337	741.1	24	18	17	00	13.5	741.1	9.9131	9.9131	

San Pedro

Niguel

Table A2. (continued)

Time		T		P		V		Time		T		P		V		
dy	hr mn sc	deg C	mmHg	deg C	mmHg	deg C	mmHg	dy	hr mn sc	deg C	mmHg	deg C	mmHg	dy	hr mn sc	
25	02 43 00	2.3	618.8			26	00 20 00	5.5	617.3	6.1694		24	04 45 00	8.5	719.3	8.3828
25	02 51 00	2.4	618.8		4.7315							24	05 00 00	8.5	719.3	8.2263
25	03 00 00	2.3	618.8									24	05 30 00	8.0	719.3	8.0724
25	03 15 00	1.7	618.8									24	06 37 00	8.0	719.3	7.8313
25	03 27 00	1.5	618.8									24	08 28 00	8.6	719.3	7.6840
25	04 15 00	1.1	618.8		4.5811							24	10 05 00	9.0	718.6	7.6258
25	04 25 00	1.0	618.8									24	11 01 00	8.0	718.6	7.3403
25	05 15 00	.5	618.8									24	12 00 00	8.0	718.6	7.3403
25	05 25 00	.8	618.8									24	13 10 00	8.0	718.6	7.1737
25	06 15 00	1.8	618.8									24	14 00 00	7.5	717.8	7.0545
25	06 23 00	2.1	618.8		4.5811							24	15 02 00	7.0	717.8	7.0645
25	06 26 00	2.0	618.8									24	15 03 00	8.0	718.6	7.4534
25	06 35 00	1.9	618.8									24	16 33 00	8.6	718.6	7.6548
25	06 37 00	1.9	618.8									24	17 31 00	11.5	718.6	8.4778
25	06 50 00	2.1	618.8									24	18 29 00	13.2	717.8	9.7318
25	07 15 00	2.3	618.8									24	19 34 00	15.0	717.1	9.8402
25	07 25 00	2.8	618.1		4.3764							24	20 30 00	16.5	716.3	9.7318
25	08 15 00	.6	618.1									24	21 30 00	15.5	716.3	9.0350
25	08 20 00	.2	618.1									24	22 30 00	16.0	715.5	9.5332
25	09 20 00	.1	618.1									24	23 30 00	14.5	715.6	9.0350
25	10 15 00	1.1	617.3									25	00 30 00	12.0	715.6	8.9724
25	10 20 00	1.9	617.3									25	01 30 00	9.5	715.6	8.0724
25	10 23 00	1.8	617.3		4.2774							25	02 36 00	8.5	715.6	7.9210
25	10 35 00	1.6	617.3									25	03 30 00	8.0	715.6	7.6258
25	10 38 00	1.7	617.3									25	04 35 00	8.5	715.6	7.8610
25	10 50 00	1.8	617.3									25	05 30 00	9.5	715.6	8.2885
25	11 15 00	2.1	617.3									25	06 35 00	8.2	715.6	7.0645
25	11 20 00	2.1	617.3									25	07 30 00	7.5	714.8	7.2012
25	12 15 00	.8	616.6									25	08 32 00	8.0	714.1	6.0678
25	12 20 00	.3	616.6		3.8100							25	09 30 00	9.0	713.3	6.3894
25	12 23 00	.4	616.6		4.3764							25	10 31 00	10.0	713.3	6.1935
25	13 15 00	.6	617.3									25	11 30 00	7.5	713.3	6.6678
25	13 20 00	.5	617.3									25	12 31 00	7.5	713.3	6.7978
25	14 20 00	-.3	617.3		4.3764							25	13 35 00	7.0	714.1	6.4354
25	15 20 00	1.9	618.1									25	14 29 00	7.0	714.1	6.0028
25	16 20 00	4.7	618.1									25	15 32 00	9.3	714.8	7.5969
25	17 20 00	5.5	618.8									25	16 32 00	11.0	715.6	8.5058
25	18 20 00	6.2	618.8		6.0500							25	17 33 00	17.0	715.6	9.2050
25	19 20 00	7.7	618.1									25	18 33 00	14.4	714.8	8.5418
25	20 20 00	8.3	617.3		6.2908							25	19 30 00	15.5	714.1	8.2263
25	21 20 00	9.4	617.3									25	20 35 00	18.0	713.3	8.3828
25	22 20 00	8.8	617.3									25	21 45 00	18.5	712.6	7.9210
25	23 20 00	6.8	617.3									25	22 33 00	20.0	712.6	7.6840
25	23 20 00	6.8	617.3									26	00 35 00	16.5	713.3	7.4818

San Juan

Table A3. Group Index of Refraction at End Points

Time		n	Time		n	Time		n	Time		n
dy	hr mn sc		dy	hr mn sc		dy	hr mn sc		dy	hr mn sc	
Mt. Wilson											
22	12 08 01	1.00024386	24	13 54 08	1.00025008	26	01 08 09	1.00024528	24	09 00 00	1.00027267
22	13 08 54	1.00024473	24	14 28 00	1.00025008	27	21 13 23	1.00024919	24	10 00 00	1.00027286
22	14 53 40	1.00024414	24	14 54 16	1.00025008				24	11 00 00	1.00027296
22	15 59 57	1.00024414	24	15 53 54	1.00025040				24	12 00 00	1.00027276
22	16 31 16	1.00024327	24	16 41 49	1.00024858				24	13 00 00	1.00027296
22	16 57 27	1.00024414	24	17 53 26	1.00024796				24	14 00 00	1.00027325
22	17 59 44	1.00024272	24	19 06 29	1.00024679				24	15 00 00	1.00027365
22	19 14 19	1.00024071	24	19 55 54	1.00024679				24	16 00 00	1.00027315
22	21 57 23	1.00024183	24	20 49 38	1.00024558				24	17 00 00	1.00027198
22	22 25 11	1.00024129	24	21 54 25	1.00024411				24	18 00 00	1.00027063
22	23 02 15	1.00024183	24	22 27 53	1.00024411				24	19 00 00	1.00026958
23	00 00 56	1.00024269	24	22 52 51	1.00024411				24	20 00 00	1.00026747
23	00 28 23	1.00024355	24	23 55 10	1.00024588				24	21 00 00	1.00026545
23	01 03 14	1.00024355	25	00 34 16	1.00024499				24	22 00 00	1.00026738
23	02 01 37	1.00024442	25	02 00 11	1.00024766				24	23 00 00	1.00026614
23	02 24 05	1.00024442	25	03 03 19	1.00024857				25	00 00 00	1.00026773
23	02 48 26	1.00024529	25	03 55 51	1.00024948				25	01 00 00	1.00027128
23	04 13 00	1.00024529	25	04 32 31	1.00024857				25	02 00 00	1.00027178
23	04 53 34	1.00024618	25	05 54 44	1.00024857				25	03 00 00	1.00027187
23	05 57 22	1.00024649	25	06 28 44	1.00024857				25	04 00 00	1.00027254
23	06 37 07	1.00024618	25	07 01 06	1.00024857				25	05 00 00	1.00027215
23	06 55 29	1.00024590	25	07 56 42	1.00024919				25	06 00 00	1.00027187
23	07 52 58	1.00024590	25	08 36 19	1.00024887				25	07 00 00	1.00027256
23	08 20 32	1.00024590	25	09 48 16	1.00024796				25	08 00 00	1.00027166
23	08 54 34	1.00024590	25	10 28 22	1.00024706				25	09 00 00	1.00027175
23	09 56 13	1.00024679	25	11 00 51	1.00024678				25	10 00 00	1.00027195
23	10 29 17	1.00024679	25	11 59 30	1.00024859				25	11 00 00	1.00027195
23	10 55 37	1.00024736	25	12 34 14	1.00024768				25	12 00 00	1.00027254
24	04 06 03	1.00025040	25	13 57 00	1.00024678				25	13 00 00	1.00027148
24	04 22 39	1.00025132	25	14 26 09	1.00024768				25	14 00 00	1.00027205
24	04 55 29	1.00025040	25	14 56 49	1.00024796				25	15 00 00	1.00027227
24	05 56 14	1.00025040	25	15 55 10	1.00024738				25	16 00 00	1.00027244
24	06 34 27	1.00025132	25	16 36 22	1.00024649				25	17 00 00	1.00027660
24	07 04 10	1.00025040	25	17 55 39	1.00024471				25	18 00 00	1.00026945
24	07 51 41	1.00025132	25	18 45 58	1.00024364				25	19 00 00	1.00026802
24	08 31 26	1.00025132	25	19 05 52	1.00024352				25	20 00 00	1.00026559
24	09 46 20	1.00025040	25	19 55 15	1.00024265				25	21 00 00	1.00026517
24	10 28 48	1.00025100	25	20 31 54	1.00024265				25	22 00 00	1.00026355
24	11 00 43	1.00025132	25	21 06 50	1.00024179				25	23 00 00	1.00026180
24	11 55 50	1.00025132	25	21 54 44	1.00024238				26	00 00 00	1.00026540
24	12 34 12	1.00025100	25	22 32 53	1.00024152						
San Pedro											
			24	05 00 00	1.00027286				22	10 21 00	1.00027425
			24	06 00 00	1.00027276						
			24	07 00 00	1.00027275						
			24	08 00 00	1.00027255						

Table A3. (continued)

Time		n	Time		n	Time		n	Time		n								
dy	hr	mn	sc	dy	hr	mn	sc	dy	hr	mn	sc								
24	05	45	00	25	02	43	00	1.00024949	1.00024679	26	00	20	00	1.00024337	24	04	45	00	1.00028056
24	06	25	00	25	02	51	00	1.00024940	1.00024670	24	06	00	00	1.00028056	24	06	00	00	1.00028056
24	06	40	00	25	03	00	00	1.00024931	1.00024679	24	06	30	00	1.00028056	24	06	30	00	1.00028056
24	07	40	00	25	03	15	00	1.00024944	1.00024733	24	06	37	00	1.00028056	24	06	37	00	1.00028056
24	08	20	00	25	03	27	00	1.00024935	1.00024751	24	06	28	00	1.00028056	24	06	28	00	1.00028056
24	09	20	00	25	04	15	00	1.00024952	1.00024787	24	06	20	00	1.00028056	24	06	20	00	1.00028056
24	10	20	00	25	04	25	00	1.00024907	1.00024796	24	11	01	00	1.00028056	24	11	01	00	1.00028056
24	11	20	00	25	05	15	00	1.00024943	1.00024842	24	12	53	00	1.00028056	24	12	53	00	1.00028056
24	12	20	00	25	05	25	00	1.00024907	1.00024815	24	13	10	00	1.00028056	24	13	10	00	1.00028056
24	13	20	00	25	06	15	00	1.00024907	1.00024724	24	14	00	00	1.00028056	24	14	00	00	1.00028056
24	14	20	00	25	06	23	00	1.00024816	1.00024697	24	15	02	00	1.00028056	24	15	02	00	1.00028056
24	15	20	00	25	06	26	00	1.00024690	1.00024706	24	16	03	00	1.00028056	24	16	03	00	1.00028056
24	16	20	00	25	06	35	00	1.00024780	1.00024715	24	16	33	00	1.00028056	24	16	33	00	1.00028056
24	17	20	00	25	06	37	00	1.00024692	1.00024715	24	17	02	00	1.00028056	24	17	02	00	1.00028056
24	18	20	00	25	06	50	00	1.00024700	1.00024697	24	18	29	00	1.00028056	24	18	29	00	1.00028056
24	18	37	00	25	07	15	00	1.00024665	1.00024697	24	19	34	00	1.00028056	24	19	34	00	1.00028056
24	19	20	00	25	07	25	00	1.00024513	1.00024607	24	20	30	00	1.00028056	24	20	30	00	1.00028056
24	20	00	00	25	08	15	00	1.00024495	1.00024805	24	21	36	00	1.00028056	24	21	36	00	1.00028056
24	20	15	00	25	08	20	00	1.00024417	1.00024841	24	22	30	00	1.00028056	24	22	30	00	1.00028056
24	20	30	00	25	08	24	00	1.00024316	1.00024850	24	22	30	00	1.00028056	24	22	30	00	1.00028056
24	20	40	00	25	09	20	00	1.00024298	1.00024727	24	23	30	00	1.00028056	24	23	30	00	1.00028056
24	20	50	00	25	10	15	00	1.00024281	1.00024655	25	00	30	00	1.00028056	25	00	30	00	1.00028056
24	21	00	00	25	10	20	00	1.00024169	1.00024664	25	01	30	00	1.00028056	25	01	30	00	1.00028056
24	21	05	00	25	10	23	00	1.00024253	1.00024664	25	02	36	00	1.00028056	25	02	36	00	1.00028056
24	21	15	00	25	10	35	00	1.00024219	1.00024692	25	03	30	00	1.00028056	25	03	30	00	1.00028056
24	22	00	00	25	10	38	00	1.00024150	1.00024673	25	04	35	00	1.00028056	25	04	35	00	1.00028056
24	22	15	00	25	10	50	00	1.00024133	1.00024664	25	05	39	00	1.00028056	25	05	39	00	1.00028056
24	22	20	00	25	11	15	00	1.00024142	1.00024638	25	06	35	00	1.00028056	25	06	35	00	1.00028056
24	22	23	00	25	11	20	00	1.00024090	1.00024638	25	07	30	00	1.00028056	25	07	30	00	1.00028056
24	22	32	00	25	12	15	00	1.00024228	1.00024726	25	08	32	00	1.00028056	25	08	32	00	1.00028056
24	22	35	00	25	12	20	00	1.00024253	1.00024772	25	09	30	00	1.00028056	25	09	30	00	1.00028056
24	22	45	00	25	12	23	00	1.00024305	1.00024762	25	10	31	00	1.00028056	25	10	31	00	1.00028056
24	23	15	00	25	13	15	00	1.00024436	1.00024772	25	11	30	00	1.00028056	25	11	30	00	1.00028056
24	23	35	00	25	13	20	00	1.00024471	1.00024782	25	12	31	00	1.00028056	25	12	31	00	1.00028056
25	00	15	00	25	14	20	00	1.00024502	1.00024854	25	13	35	00	1.00028056	25	13	35	00	1.00028056
25	00	20	00	25	15	20	00	1.00024560	1.00024687	25	14	25	00	1.00028056	25	14	25	00	1.00028056
25	00	25	00	25	16	20	00	1.00024578	1.00024687	25	15	32	00	1.00028056	25	15	32	00	1.00028056
25	00	29	00	25	17	20	00	1.00024537	1.00024439	25	16	32	00	1.00028056	25	16	32	00	1.00028056
25	01	15	00	25	18	20	00	1.00024635	1.00024396	25	17	33	00	1.00028056	25	17	33	00	1.00028056
25	01	20	00	25	19	20	00	1.00024644	1.00024335	25	18	33	00	1.00028056	25	18	33	00	1.00028056
25	02	15	00	25	20	20	00	1.00024670	1.00024178	25	19	30	00	1.00028056	25	19	30	00	1.00028056
25	02	27	00	25	21	20	00	1.00024679	1.00024095	25	20	35	00	1.00028056	25	20	35	00	1.00028056
25	02	32	00	25	22	20	00	1.00024662	1.00024001	25	21	45	00	1.00028056	25	21	45	00	1.00028056
25	02	39	00	25	23	20	00	1.00024679	1.00024052	25	22	33	00	1.00028056	25	22	33	00	1.00028056
25	02	39	00	25	23	20	00	1.00024224	1.00024224	26	00	35	00	1.00028056	26	00	35	00	1.00028056

San Juan

Table A4. Time-of-Flight Ratios

Castro		San Pedro		Niquel		Santiago		San Juan	
dy	hr mn sc	dy	hr mn sc	dy	hr mn sc	dy	hr mn sc	dy	hr mn sc
22	10 04 29	22	10 18 55	24	04 20 32	22	10 41 41	22	10 51 17
22	12 02 41	22	12 21 52	24	06 19 58	22	12 43 11	22	12 51 51
22	14 05 43	22	14 15 03	24	06 46 28	22	14 34 32	22	14 48 04
23	00 09 40	22	18 23 39	24	08 18 26	22	22 49 55	22	18 55 03
23	02 09 25	24	04 20 40	24	10 15 13	23	00 41 06	22	22 54 50
23	06 05 03	24	06 16 19	24	10 40 16	23	04 33 04	22	05 47 01
24	06 08 46	24	06 51 04	24	14 15 10	23	06 39 34	23	08 47 14
24	06 58 17	24	08 09 40	24	14 40 18	23	08 39 44	24	04 43 14
24	08 00 19	24	10 10 03	24	16 18 20	24	04 40 08	24	05 29 45
24	09 59 54	24	10 45 34	25	02 21 58	24	06 25 43	24	06 36 37
24	10 55 03	24	12 10 04	25	02 48 49	24	06 41 31	24	08 25 49
24	12 00 58	24	14 11 30	25	10 16 05	24	08 22 17	24	12 25 00
24	14 01 34	24	14 45 60	25	10 41 13	24	10 21 13	24	14 25 20
24	14 55 05	25	02 13 18	25	02 13 18	24	10 35 15	24	14 30 04
24	16 01 03	25	02 53 27	25	02 53 27	24	12 20 03	24	16 22 54
24	18 00 06	25	04 09 53	25	04 09 53	24	14 20 03	25	02 33 03
24	18 57 39	25	06 10 05	25	06 10 05	24	14 35 11	25	02 36 56
24	22 44 42	25	06 45 43	25	06 45 43	24	16 29 53	25	04 25 60
25	02 05 25	25	08 11 36	25	08 11 36	24	20 18 04	25	06 32 42
25	02 58 04	25	10 10 16	25	10 10 16	25	00 25 13	25	08 23 56
25	04 00 52	25	10 45 23	25	10 45 23	25	02 29 30	25	10 25 11
25	06 01 17	25	12 10 30	25	12 10 30	25	02 39 51	25	10 30 03
25	06 55 21	25	14 15 11	25	14 15 11	25	04 22 37	25	12 25 03
25	08 04 49	25	14 40 42	25	14 40 42	25	06 22 51	25	16 31 55
25	10 01 53	25	14 61 14	25	14 61 14	25	06 35 48	25	20 25 59
25	10 55 08	25	15 20 08	25	15 20 08	25	08 20 32	25	22 28 50
25	12 04 05	25	14 27 7	25	14 27 7	25	10 20 08	25	22 28 50
25	14 51 54	25	15 40 9	25	15 40 9	25	10 35 11	25	22 28 50
25	16 00 28	25	16 00 28	25	16 00 28	25	12 21 02	25	22 28 50
25	18 00 19	25	14 47 3	25	14 47 3	25	14 21 41	25	22 28 50
25	18 59 43	25	14 61 3	25	14 61 3	25	14 35 02	25	22 28 50
25	20 07 42	25	14 24 3	25	14 24 3	25	16 20 06	25	22 28 50
25	20 37 24	25	13 55 2	25	13 55 2	25	18 39 42	25	22 28 50
25	20 49 58	25	14 76 6	25	14 76 6	25	20 20 59	25	22 28 50
25	22 51 57	25	12 78 6	25	12 78 6	25	22 37 54	25	22 28 50
26	00 05 27	25	12 96 1	25	12 96 1	26	00 26 53	25	22 28 50

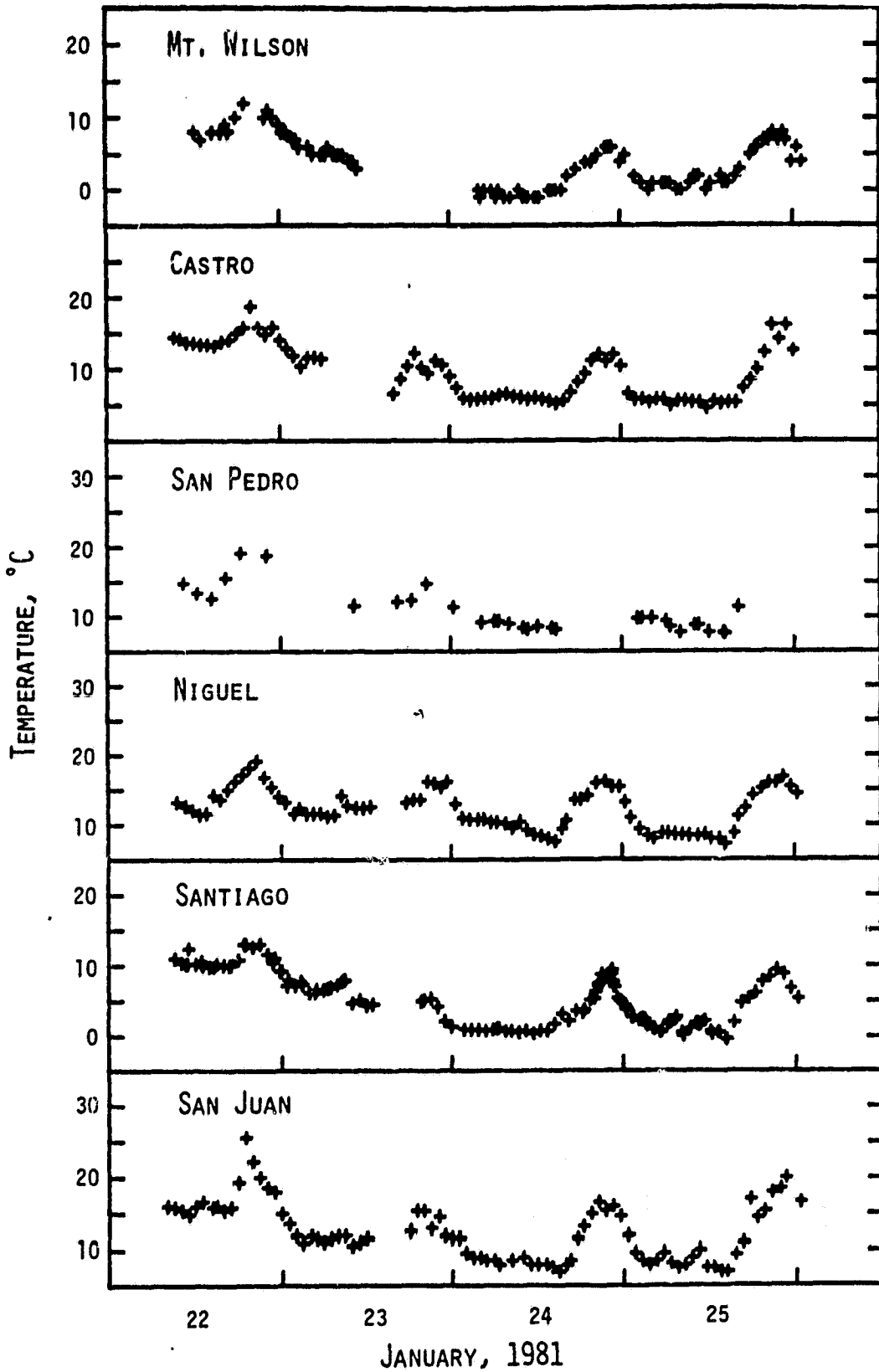


Fig. A1. Observed atmospheric temperature.

ORIGINAL PAGE IS
OF POOR QUALITY

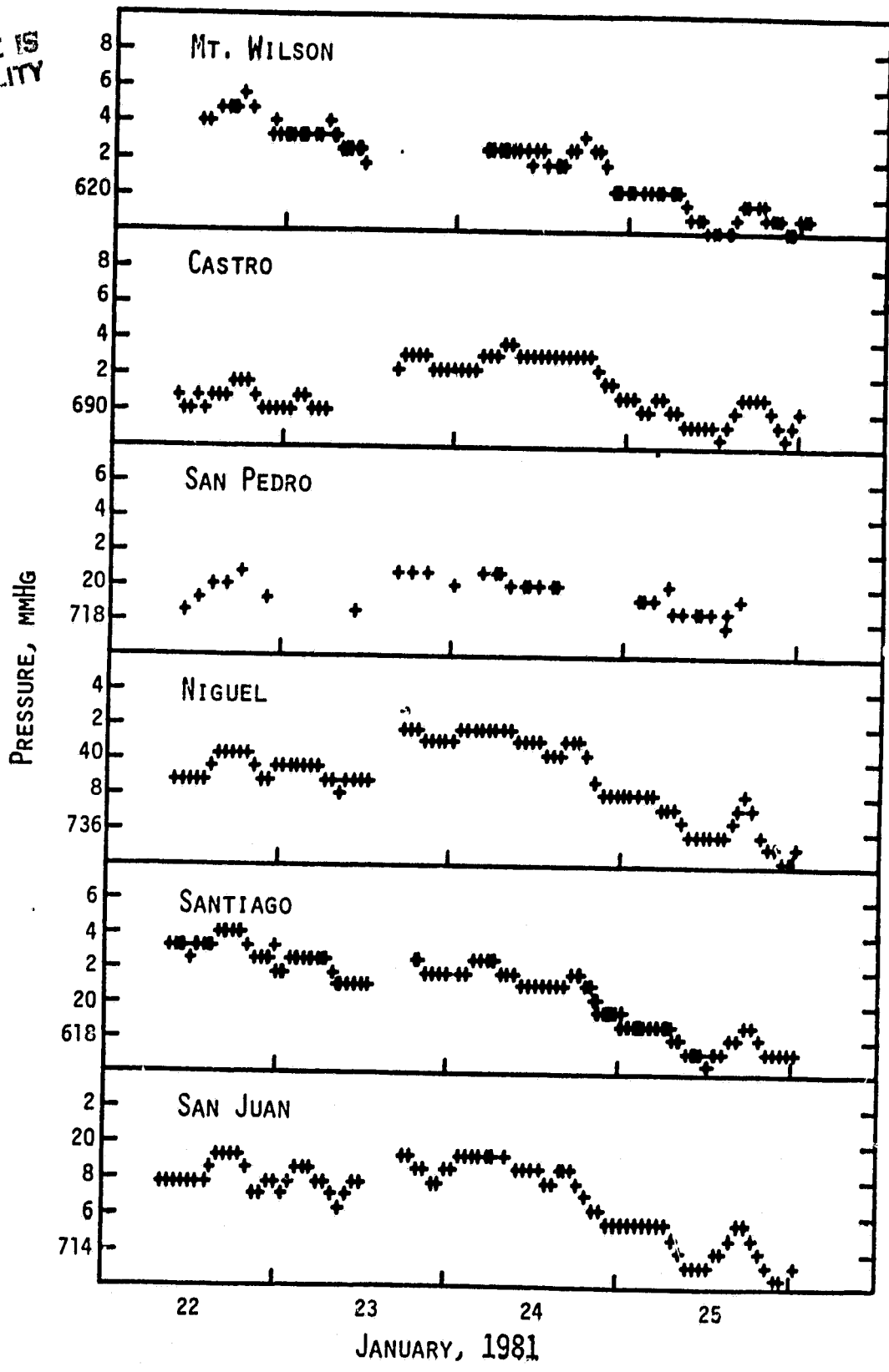


Fig. A2. Observed atmospheric pressure.

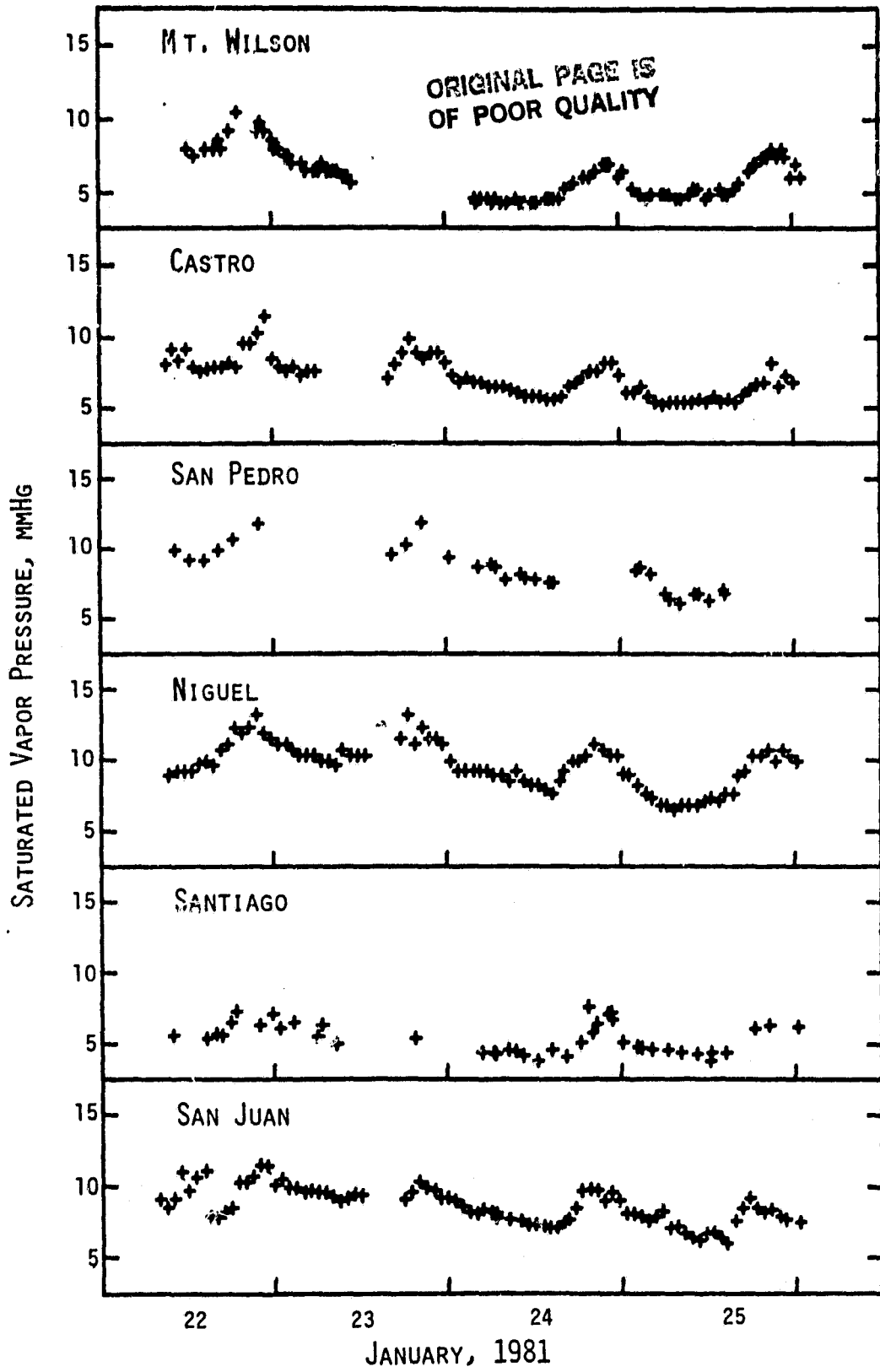


Fig. A3. Saturated vapor pressure.